# Densification Behaviour and Structural Properties of Niobium and Lanthanum-doped Lead Zirconate Titanate and Lead Barium Zirconate Ferroelectrics for Low-donor Dopants Concentrations

**David Bahati[1,2] and Ismael N. Makundi[1]**
*[1]Physics Department, University of Dar es Salaam, P. O. Box 35063 Dar es Salaam*
*[2]Physics Department, University of Dodoma, P. O. Box 338 Dodoma*
*E-mail address: ismakundi@udsm.ac.tz*

## Abstract

In this paper we report the densification behaviour and structural properties of niobium and lanthanum-doped lead zirconate titanate (PZT) and lead barium zirconate (PBZ) ferroelectrics for low additive concentrations (0–2%). The PZT materials were calcined at 800 °C and sintered at 1200 °C while the PBZ materials were calcined at 850 °C and sintered at 1250 °C. Densification behaviour revealed that materials with lanthanum or niobium additives of greater than 0.5% for PZT and 0.2% for PBZ achieved complete densification. A strong distortion was observed in lattice parameters for lower dopants in which PBZ doped materials showed higher lattice distortions than PZT doped materials. The grain sizes decreased with increasing dopants concentrations for PZT while it increased with increasing dopants concentrations for PBZ materials.

## Introduction

Ferroelectric materials are subgroup of piezoelectric materials, where a spontaneous polarization exists that can be reoriented by application of DC electric field (Jalaja and Dutta 2015). For piezoelectric applications, ferroelectrics are preferred since they can be poled to enhance the piezoelectric functionality. The most suitable piezoelectric materials for applications in actuators are therefore ferroelectric ceramics (Uchino 2008). Piezoelectric ceramics are widely used in sensors, actuators and transducers that are important in diverse fields such as industrial process control, environmental monitoring, communications, information systems and medical instrumentation, depending on application requirements and technology. They can be used in the forms of bulk ceramics, thin films, multi-layers, single crystals, polymers and composites (Setter 2002).

Useful properties of piezoelectric ceramics depend on their composition and crystal structures, temperature and dopants, which explain the degree of their response to the applied mechanical stress or electric field. Barium titanate ($BaTiO_3$) was the first piezoelectric ceramic material discovered and lead zirconate titanate (PZT) is by far the most widely used piezoelectric ceramic. Another well-known piezoelectric ceramic is potassium niobate ($KNbO_3$) (Setter 2002, Moulson and Herbert 2003), which has recently drawn interest as a potential lead-free replacement to PZT.

The PZT ferroelectric ceramics are used in applications such as transducers, actuators and sensors. This is due to the fact that PZT compositions possess advantageous combination of properties such as high piezoelectric and electromechanical coupling coefficients; high Curie point ($T_C$) which permits a high temperature of operation (above 200 °C) and they can be easily poled.

144

Also PZT materials possess a wide range of dielectric constants, relatively lower sintering temperatures and form solid solution compositions with many different constituents, thus allowing a wide range of achievable properties (Haertling 1999). It is important to improve PZT ferroelectric materials in order to obtain good and reproducible ferroelectric materials for desired applications. One way to achieve such improvements and to tune the properties of ceramics for particular applications is by doping.

Doped PZT ceramics are mainly divided into the "soft" and "hard" PZTs, which are normally prepared by substituting the A-site or B-site ions with donor and acceptor dopants, respectively (Wongdamnern et al. 2008). Soft lead zirconate titanate (PZT) and lead barium zirconate (PBZ) are formed when the charge on the cation is larger than that which it replaces, while hard PZT and PBZ materials are formed when the charge on the

cation is smaller than that of the ion which it replaces. The donor dopants enhance both the dielectric and piezoelectric properties at room temperature and show symmetric hysteresis loops with good "squareness" and lower coercivity with respect to the high fields. The acceptor dopants in general reduce both dielectric and piezoelectric properties; they give rise to highly asymmetric hysteresis response, larger coercivity and higher electrical and mechanical quality factor (Jin 2011). Here we report the effect of low additive concentrations of Nb and La on the densification behaviour and structural properties of PZT and PBZ ferroelectric ceramics.

**Materials and Methods**

The solid state reaction (mixed oxide) method was used in the fabrication process. The main steps of the mixed oxide route are summarized in Figure 1.
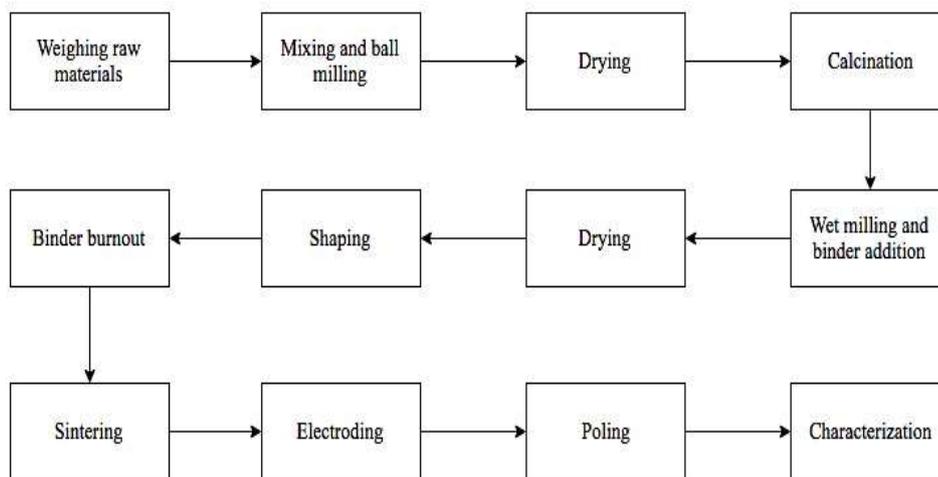


**Figure 1:** The flow chart showing the steps of the processing of PZT and PBZ (Richerson 2006).

The oxides used in this study were of high purity grade of 99.99% PbO (Sigma-Aldrich USA), 99.99% $ZrO_2$ (Sigma-Aldrich UK), 99.8% $TiO_2$, 99.99% $Nb_2O_5$ and 99.95% $BaCO_3$ (Alfa Aesar UK). The powder oxides

were weighed by using a digital weighing machine (mittler PM 200) and mixed in their stoichiometric proportions according to the following formula:
$(Pb_{0.77}Ba_{0.23})(Zr_{1-x}Nb_x)O_3, (Pb0.77_{1-x}Ba0.23)La_xZrO_3,$
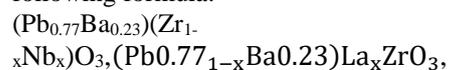
$Pb_{1-\frac{x}{2}}V_{\frac{x}{2}}$ and $Pb_{1-x}La_x\left(Zr_{\frac{1}{2}}Ti_{\frac{1}{2}}\right)O_3$ for PBZ and PZT,

where $x = 0$, 0.0005, 0.001, 0.0015, 0.002, 0.005, 0.01, 0.0155 and 0.0 2 for PBZ and $x = 0$, 0.001, 0.002, 0.005, 0.01 and 0.02 for PZT.

In order to eliminate aggregates and reduce the particle size, the powder oxides were wet milled together in their proper proportions using zirconium dioxide ball-mills and isopropanol alcohol in the mixing machine for 2 hours. The wet mixed wet-milled oxides were evaporated to dry and then sieved through a sieving machine for 15 minutes. The dried powder was put in zirconium dioxide crucible for calcination process. Since lead oxide is volatile, the crucibles were covered in order to minimize lead loss due to vaporization. To compensate for lead loss during calcination and sintering processes, 1% by weight excess of PbO was included in the weighing process. The dried powder was calcined at 800 °C for PZT and 850 °C for PBZ for 2 hours in the furnace Lenton Thermal Designs LTD, serial number 2991 as summarized in Table 1.

**Table 1:** Calcination process of PZT and PBZ samples

| Heating rate (°C/min) | Calcining temperature (°C) | Holding time (hours) | Cooling rate (°C/min) | Final temperature (°C) |
|---|---|---|---|---|
| 5 | 800 for PZT 850 for PBZ | 2 | 5 | 30 |

Due to high calcining temperature (800 °C for PZT and 850 °C for PBZ), calcined sample usually undergoes a limited amount of sintering, so must be milled to give a powder. Therefore, in order to ensure homogeneity, the calcined powder was then mixed with isopropanol and a 5% by weight of polyvinyl alcohol (PVA) water solution was added as a binder to increase the plasticity of the powders. The entire mixture was then wet-milled for 24 hours using zirconium dioxide ball-mills in Planetary Ball mill (QM 3SP2) machine and then evaporated to dry in order to prepare it for pressing to form pellets.

Shaping of the powder was carried out on a pressing machine, type model PW10.

About 0.300 g of the dried powder was pressed at a pressure of 41.6 MPa and 80 MPa for PZT and PBZ, respectively each time to form a disk pellet. The pellets were then kept at a temperature of 600 °C for 6 hours in order to evaporate the binder. Before the sintering process, the pellets were weighed in order to be able to determine the amount of lead loss after the sintering process. In all the samples, weight losses were found to be less than 0.3%. The pellet samples were sintered at a temperature of 1200 °C for PZT and 1250 °C for PBZ for 2 hours as summarized in Table 2.

**Table 2:** Sintering process of PZT and PBZ samples

| Heating rate (°C/min) | Sintering temperature (°C) | Holding time (hours) | Cooling rate (°C/min) | Final temperature (°C) |
|---|---|---|---|---|
| 5 | 1200 for PZT and 1250 for PBZ | 2 | 5 | 30 |

The theoretical densities of the ceramics were calculated according to the relation (1) (Askeland and Wright 2015);

$$\rho_{theo} = \frac{M_r Z}{N_A V_{cell}} \qquad (1)$$

where $N_A$ is the Avogadro number,
$V_{cell}$ is the volume of the unit cell,
$M_r$ is molar mass of PZT or PBZ,
$Z$ is the number formula units contained in one unit cell (for PZT, PBZ and all perovskites $Z = 1$).

The volume of the unit cell was calculated from the lattice parameter extracted from XRD data collected on the sintered ceramics. The geometrical densities of the ceramics after sintering were calculated from the ratio between their weight and the geometrical volume given by equation (2) (Kingery et al. 1976);

$$\rho = \frac{\rho_{geo}}{\rho_{theo}} \qquad (2)$$

where $\rho$ is the relative density,
$\rho_{geo}$ is the measured density,
$\rho_{theo}$ is the theoretical density.

## Results and Discussion
In this section, the results for each property are presented and discussed separately.

## Density
Low relative density was shown by 0.05, 0.1 and 0.15% niobium doped PBZ materials and only pure samples and compositions with dopant concentrations ranging from 0.2 to 2% revealed complete densification in PBZ materials. For the PZT materials, complete densification was shown by pure samples and samples with dopant concentrations between 0.5 and 2%. The changes in the relative density in PBZ (comparing the samples with the highest and with the lowest density) are bigger compared to PZT as shown in Figure 2. Changes for PBZ were about 18% between the pure sample and the sample with 0.15% Nb and about 7% between pure and 0.1% of lanthanum. On PZT, the observed changes were 3% and 2.5% for Nb and La doping, respectively. For all the samples, the final relative densities were greater than 95% for PZT and 80% for PBZ.

Lead barium zirconate and lead zirconate titanate possess two ions, Pb and O, which are quite volatile at the sintering temperature. Since the equilibrium vapour pressures of Zr, Ba, Ti and their oxides are low at 1250 °C, these components do not evaporate readily. This implies that the material may become substantially Pb deficient if no other charge-balance mechanism is operative. This leads to the conclusion that, in the pure material, some ionic vacancies are present due the solid-state processing method. These vacancies are needed to obtain sufficiently high volume diffusion and lead to the high density (97.6% for PBZ and 97.5% for PZT) as shown in Figure 2.
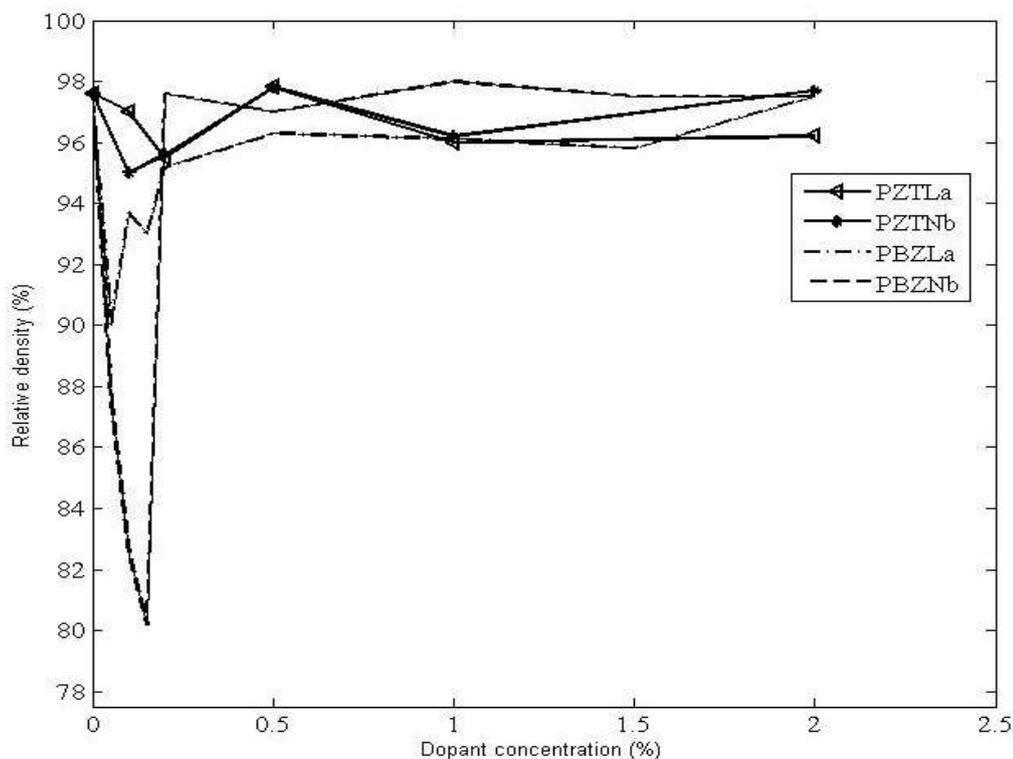
**Figure 2:** Relative density as function of dopants concentrations.

To explain the drastic decrease in densification at small concentrations of dopant, we propose that different mechanisms are involved for low and high quantities of dopants. The number of existing lead vacancies may be partially compensated by the dopants for samples with low additive contents (< 0.2 mol%). In this way, for very low quantities of niobium, part of dopant ions might occupy the A site of the perovskite instead of the expected B site. With a further increase of additive content, the Nb ions will substitute the Zr ions at the B site of the perovskite structure.

Both un-doped and doped samples contain lead vacancies, which are conducive for effective densification. The idea that the number of oxygen vacancies is reduced in Nb and La doped materials apparently does not affect much the densification process (Figure 2). What happens at low concentration of

donor dopant to reduce densification? The anomaly happens only with donor but not acceptor dopants. This indicates that the phenomenon is linked to formation of lead and oxygen vacancies, which are favoured by donor and acceptor dopants, respectively (Zuo et al. 2009).

Let us assume that at low concentration of donor dopant (< 0.2 mol%), a fraction of the existing lead vacancies is filled with the doping cations. This would lead to compensation of the Nb partially by B-site vacancies ($V_{Zr}$) and partially by A site vacancies ($V_{Pb}$) and in the case of La, to decrease the number of Pb vacancies. Since B site vacancies are expected to be less mobile than Pb vacancies, the reduction in concentration of $V_{Pb}$ would decrease the volume diffusion rate and lower the relative density, which in those samples indeed reaches only 80% (values PBZ). However,

with a further increase of additive content, the Nb ions will substitute the Zr or Ti ions at the B site of the perovskite structure, and La ions the Pb site, as is the usual case. In that case, Pb vacancies are created to reach electro-neutrality, enhancing again the volume diffusion and increasing the sintered density to about 97-98% of the theoretical values.

**Lattice parameters**

The lattice parameters obtained from the XRD results were plotted as a function of dopant concentration in order to observe the behaviour of lattice constant of the unit cell of the sintered material as a function of dopant concentration. A strong distortion was observed between 0.05 to 0.2% lanthanum and niobium doped PBZ samples. However, for PZT lanthanum and niobium doped samples, a strong lattice distortion was observed between 0.1 to 0.5%. PBZ doped samples show higher lattice distortion than PZT doped samples as shown in Figure 3.
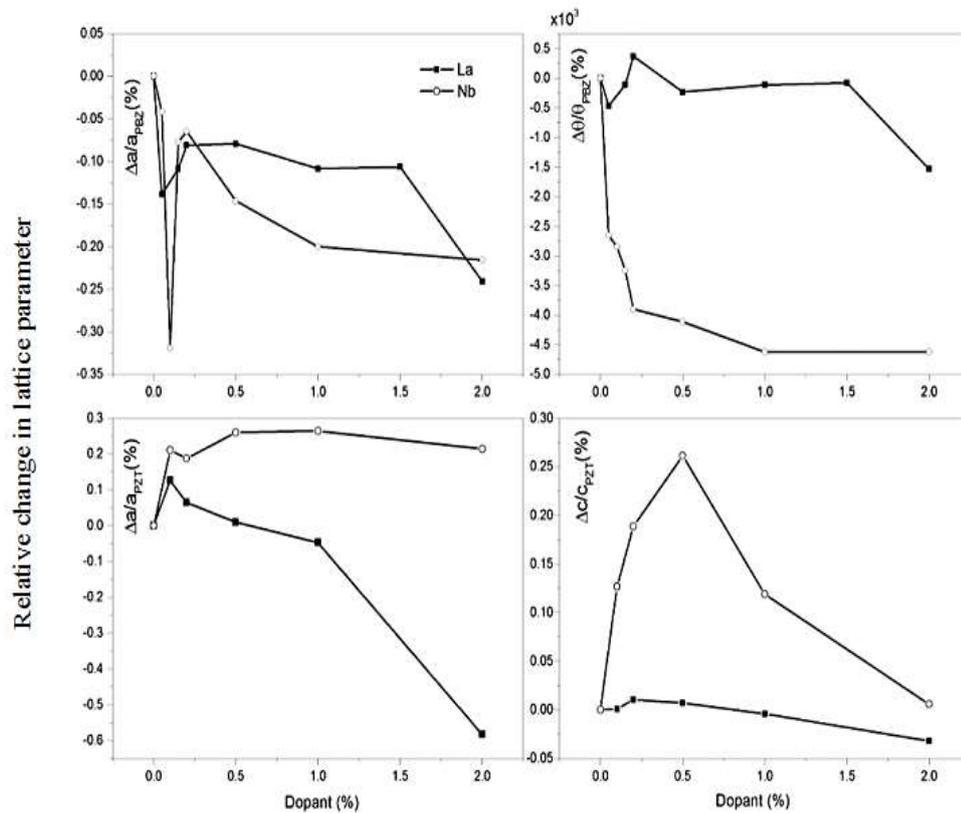


**Figure 3:** Relative changes in lattice parameters as functions of dopants concentrations for PZT and PBZ samples.

**Fracture mode**

SEM (Scanning Electron Microscope) images for fractured ceramics are shown in Figure 4. For the PZT pure samples, due to technical problems (accumulation of charge) it was necessary to deposit a carbon layer in order to reduce conductivity. Pure PZT ceramics presented mostly transgranular fracture, and it is even possible to observe ferroelectric domains, generally only visible in well-

polished surfaces. Addition of Nb dopants changes the fracture modes to a mix of both transgranular and intergranular fracture modes. Intergranular fracture mode becomes dominant at high Nb concentrations. For La samples, even small quantities of La revealed mostly intergranular fracture mode as shown in Figure 4. In the case of PBZ, all the samples presented clear intergranular fracture mode.
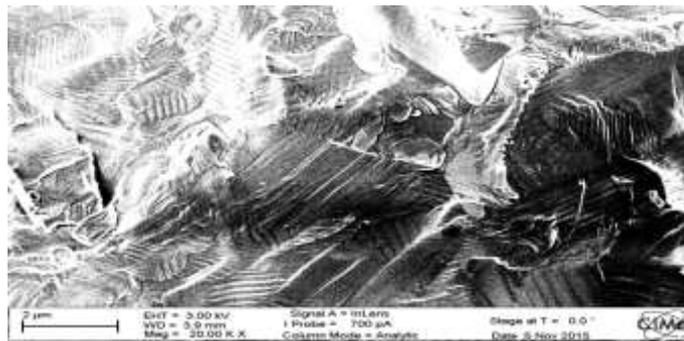

Pure PZT
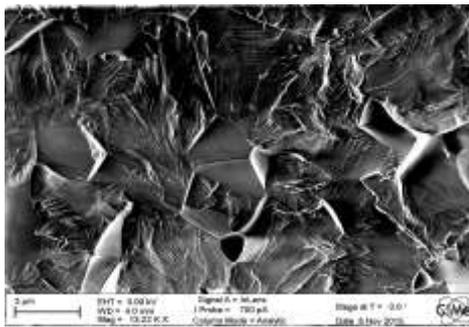

PZT 0.1% Nb
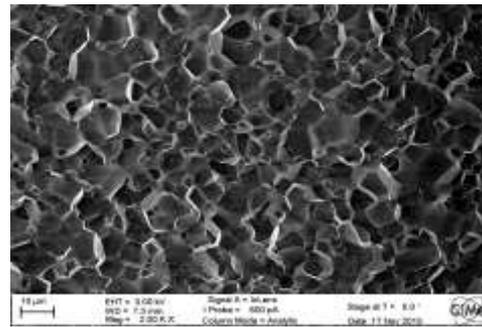

PZT 0.1% La
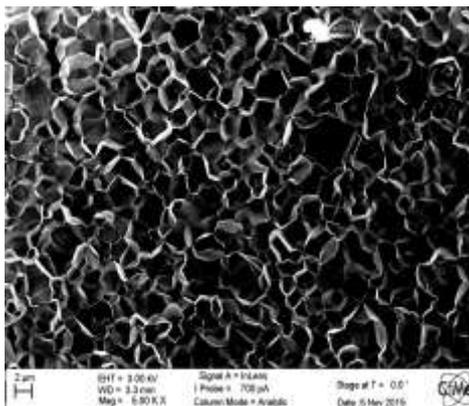

PZT 2% Nb
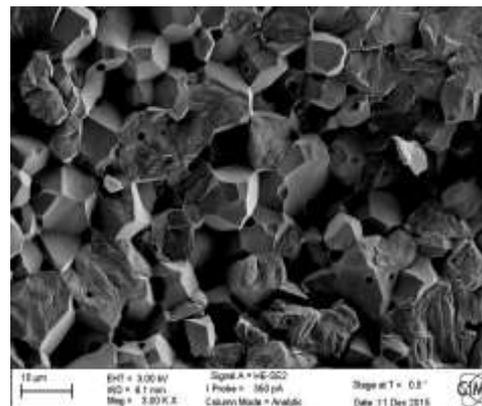

PZT 2% La

**Figure 4:** Typical SEM images of fracture samples of PZT.

**Grain size**

SEM observations of the grains were performed on all the 'surface' specimens. A number of pictures of the grains were taken in different areas (typically between 5 and 10) of each specimen, as shown in Figure 5. Grain size measurements were performed using the IMAGEJ software package. Mean grain sizes of PZT-based and PBZ-based materials versus Nb and La concentrations are reported in Figure 7.

In the case of PZT-based materials, the grain size first increased with the Nb or La content from a value of about 3.9 μm for pure PZT up to values of about 15.4 μm for PZT-0.1%Nb and 16.5 μm for PZT-0.2%La.There after the grain size decreased as the Nb or La content is further increased (more continuously in the case of La than in the case of Nb), down to values of about 2.2 μm for PZT-2% Nb and 9 μm for PZT-2% La. For Nb-doped PBZ materials grain size first decreased for lower concentrations up to about 1.35 μm at 0.1% Nb concentration and then increased continuously with increasing Nb concentrations. For La-doped PBZ materials, grain size decreased for lower concentrations up to about 1.8 µm at 0.1% La concentration where it started to increase with increasing La concentrations up to about 3.15 μm at 0.5% La before decreasing continuously with increasing La concentrations. Similar grain size dependence

on the dopant contents was also obtained by Hammer and Hoffmann (1998) on PZT-based materials containing various amounts of La, who attributed the maximum in grain size as due to a relatively high ratio of the grain growth rate to the densification rate. The main densification mechanism was volume diffusion controlled by the number of vacancies and the grain growth occurring due to surface diffusion or by evaporation condensation, the latter being certainly negligible. However, Hammer and Hoffmann (1998) concluded that the grain growth inhibition effect in PZT ceramics occurred by a solute drag mechanism that originated from chemical inhomogeneities (Zr enrichment of the shell and La enrichment in the Ti-rich core of the grain, which they observed experimentally) and not from La segregation at the grain boundaries.

Somewhat reverse results have been obtained for PBZ-based materials, as it can be seen in Figures 6 and 7. The grain sizes first decreased as the Nb or La content was increased, from a value of about 3.6 μm for pure PBZ down to values of about 1.6 μm for PBZ-0.05%Nb and 1.4 μm for PBZ-0.2% La, and then the grain size increased as the Nb or La content was further increased (more continuously in the case of La than in the case of Nb), up to values of about 2.6 μm for PBZ-2% Nb and 6 μm for PBZ-2% La.

Pure PZT

PZT 0.1% Nb

PZT 0.2% Nb

PZT 0.5% Nb

PZT 1% Nb

PZT 2% Nb

PZT 0.1% La

PZT 0.2% La
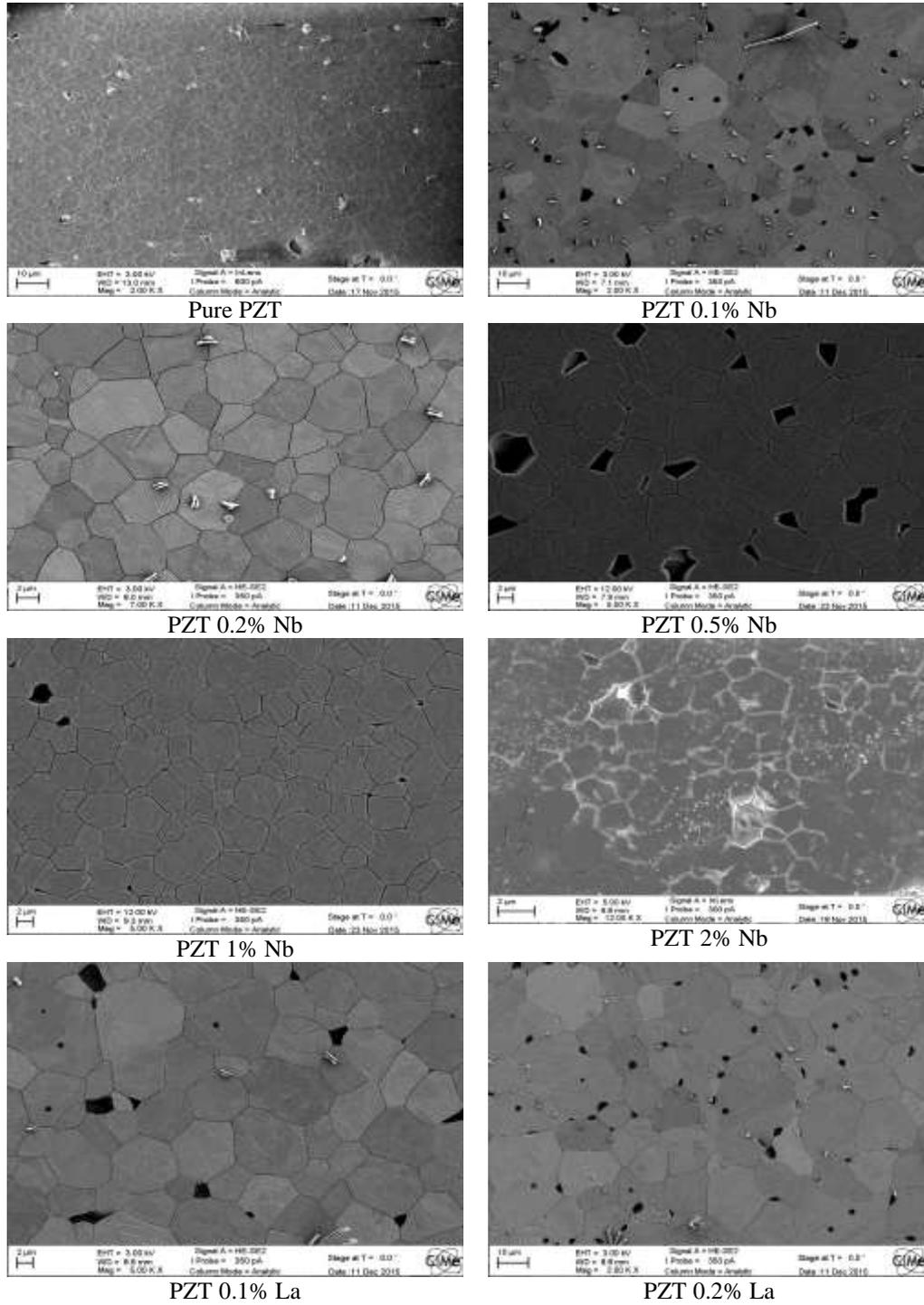
**Figure 5:** Typical SEM images of surface specimens of PZT-based samples**.**

PZT 0.5% La


PZT 1% La


PZT 2% La
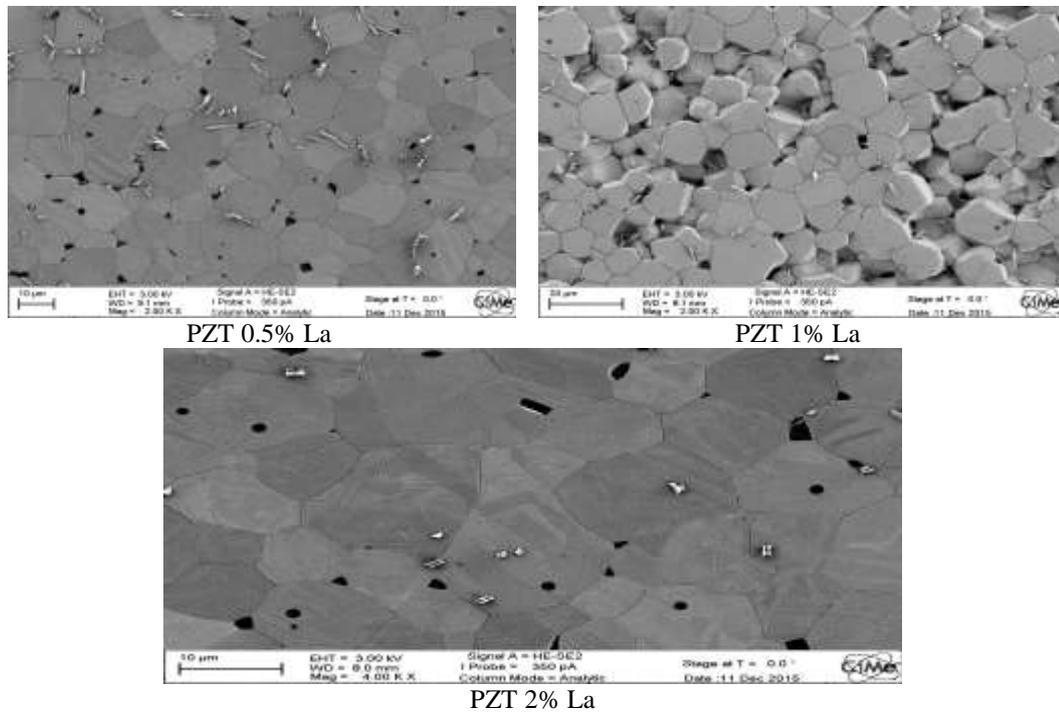
**Figure 5 (ctd):** Typical SEM images of surface specimens of PZT-based samples.


Pure PBZ


PBZ 0.05% Nb
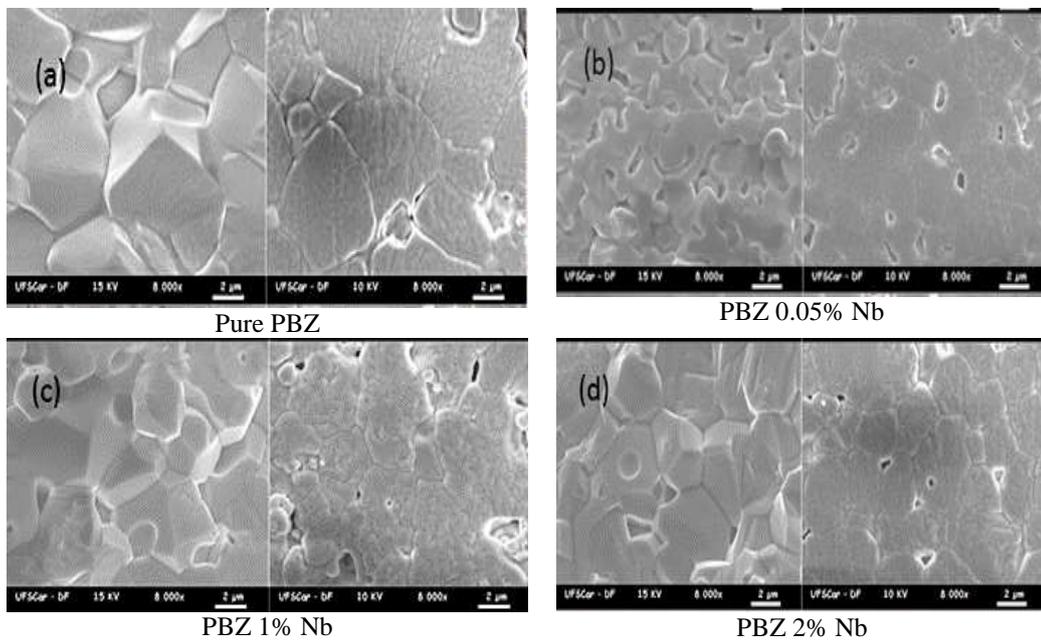

PBZ 1% Nb


PBZ 2% Nb

**Figure 6:** Typical SEM images of surface specimens of PBZ-based materials (a) pure PBZ, (b) PBZ-0.05% Nb (c) PBZ-1% Nb and (d) PBZ-2% Nb.
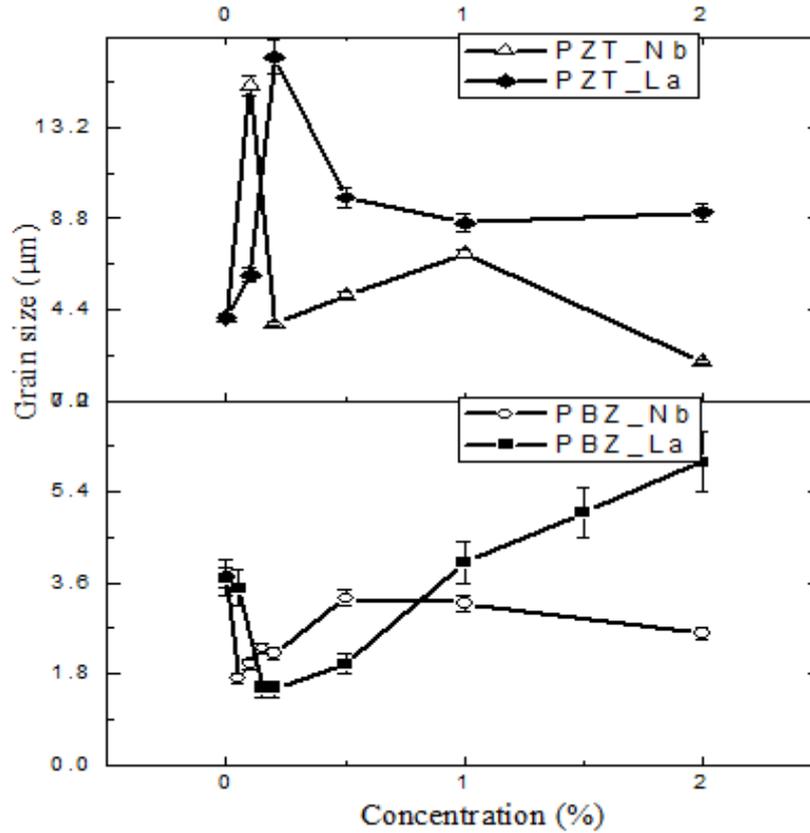
**Figure 7:** Mean grain size (µm) as function of dopants concentrations (%).

**Ferroelectric domains**

Ferroelectric domains were evidenced within the grains of all the investigated PZT-based materials. The observed domains appeared to be mostly 90° domains with typical straight walls as shown in Figure 8. However, 180° domains with a water-like contrast were also observed in a number of materials, more especially at high Nb and La concentrations. In addition, the sizes of domains were found to decrease with increasing Nb or La dopant concentrations.

Pure PZT


PZT 0.1% Nb (mostly 90°domains)


PZT 2% Nb (mostly 180°domains)


PZT 0.2% La
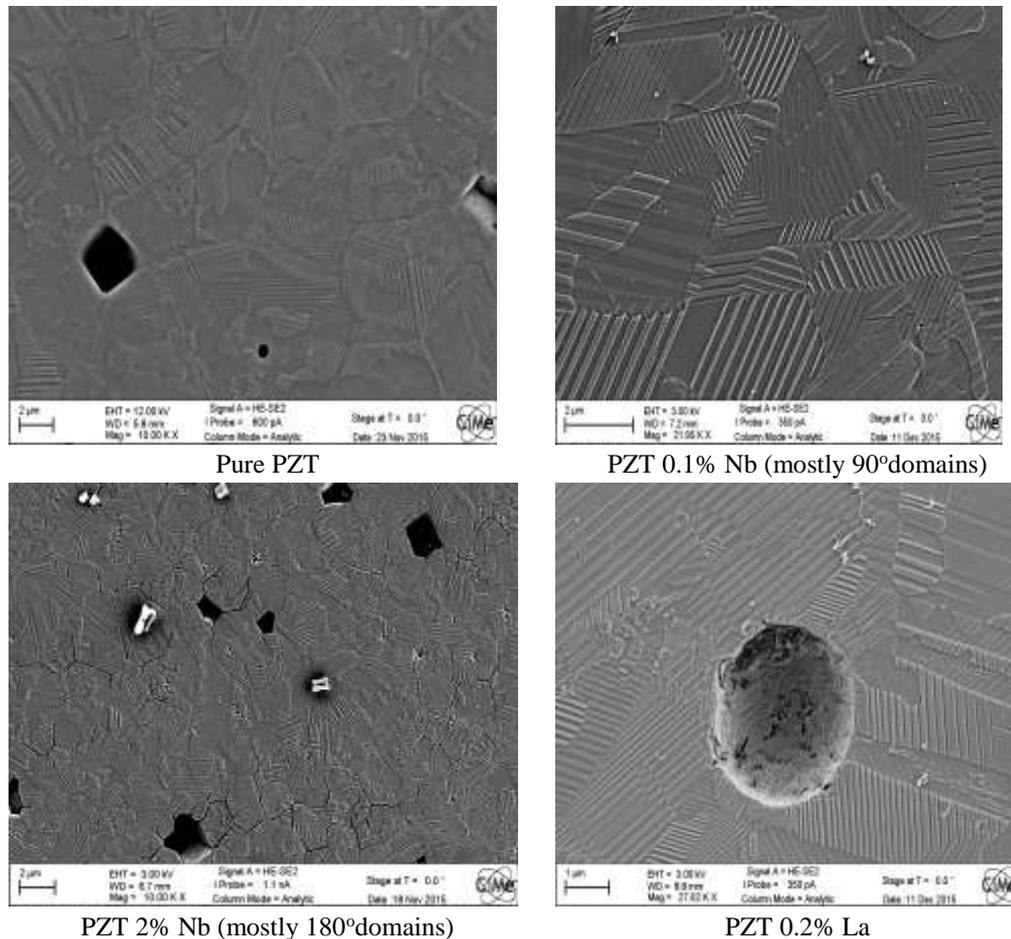
**Figure 8:** Typical SEM images of ferroelectric domains in PZT-based samples.

## Porosity

Peculiar objects with spherical shape were observed in most of the 'fracture' specimens of the PZT-based materials. They were located within the grains, as shown in Figure 9 in the case of La containing materials, or at the intersection of two or several grains (e.g., triple junctions), as also shown in Figure 9. Shade effects at the inner borders of the objects revealed that these objects are of the 'hole' type (pores) and not of the 'bubble' type. The sizes of these hole-like structures typically ranged between 1 and 5 μm. For a given dopant content, the concentration of these hole-like structures

were found generally higher in La-containing PZT specimens than in Nb-containing PZT specimens. The concentrations of these structural features were estimated to be the highest in PZT-0.1% Nb and PZT-0.2% La specimens. The presence of such hole-like structures could be eventually attributed to a too high densification rate during the sintering process, two or three grains with the same orientation growing, meeting and forming a single grain during sintering, leaving a relatively large hole-like structure at the centre of the newly formed single grain, in the case of e.g., a hole-like structure located inside a grain. Note that series of concentric

circular contrasts were often observed within the objects (hole-like structures), as it can be seen in Figure 9, which are not related to the presence of ferroelectric domains (not really visible in the case of 'fracture' specimens as they were not chemically etched) but certainly due to the formation of crystallographic facets occurring during the pore formation.



PZT 0.5% La          PZT 0.5% La

PZT 2% La            PZT 2% La
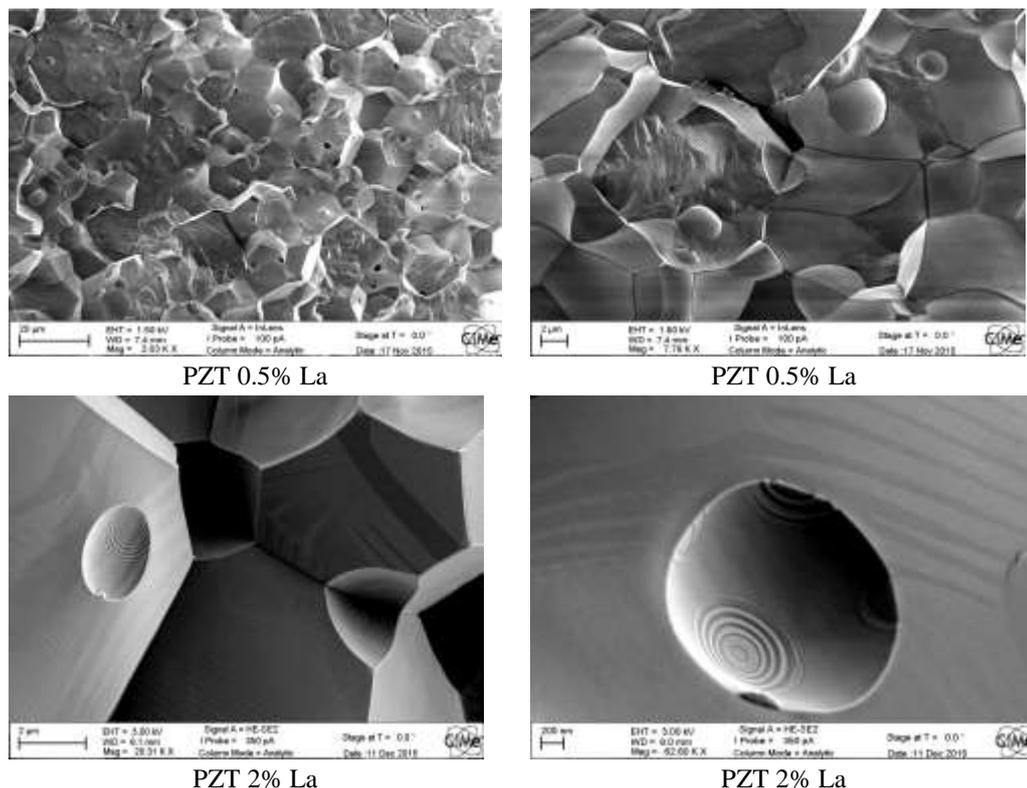
**Figure 9:** Typical SEM images of pores (hole-like structure) inside PZT-based materials.

## Conclusion

Based on these results, we propose some conditions for complete densification of PZT and PBZ-doped materials at low level of additives. In the case of PZT and PBZ-based materials a minimum dopant content of about 0.2-0.5% Nb or La was needed for allowing full sintering to occur and getting a stable structure and micro-structure properties. In addition, when the Nb or La contents were further increased above the critical amounts of about 0.2 to 0.5%, the grain sizes decreased (for PZT-based materials) or increased (for PBZ-based materials). On the other hand, the sintering temperatures of about 1200 °C and 1300 °C for 2 hours for PZT and PBZ, respectively were appropriate for complete densification.

## References

Askeland DR and Wright WJ 2015 The Science and Engineering of Materials. 7th Ed. Global Engineering. USA.

Haertling GH 1999 Ferroelectric ceramics: history and technology. *J. Am. Ceram. Soc.* 82(4): 797-818.

Hammer M and Hoffmann MJ 1998 Sintering model for mixed-oxide-derived lead zirconate titanate ceramics. *J. Am. Ceram. Soc.* 81(12): 3277-3284.

Jalaja MA and Dutta S 2015 Ferroelectrics and multiferroics for next generation photovoltaics. *Advanced Materials Letters* 6(7): 568-584.

Jin L 2011 *Broadband dielectric response in hard and soft PZT: Understanding softening and hardening mechanisms* PhD thesis. Ceramics Laboratory EPFL, Swiss Federal Institute of Technology, Lausanne, Switzerland.

Kingery WD, Bowen HK and Uhlmann DR 1976 Introduction to Ceramics. 2nd Ed. Wiley, New York.

Moulson AJ and Herbert JM 2003 Electroceramics. 2nd Ed., John Wiley and Sons Ltd, England.

Richerson DW 2006 Modern Ceramic Engineering. 3rd Ed., CRC press, USA.

Setter N 2002 Piezoelectric Materials in Devices: Extended reviews on current and emerging piezoelectric materials, technology and applications. Switzerland: Ceramics Laboratory EPFL Swiss Federal Institute of Technology.

Uchino K 2008 Piezoelectric actuators. EEExpansion from IT/robotics to ecological/energy applications. *J. Electroceram.* 20(3-4): 301-311.

Wongdamnern N, Triamnak N, Ngamjarurojana A, Laosiritaworn Y, Ananta S and Yimnirun R 2008 Comparative studies of dynamic hysteresis responses in hard and soft PZT ceramics. *Ceram. Int.* 34(4): 731-734.

Zuo R, Wang H, Ma B, and Li L 2009 Effects of $Nb^{5+}$ doping on sintering and electrical properties of lead-free $(Bi_{0.5}Na_{0.5})TiO_3$ ceramics. *J. Mater. Sci. Mater. Electron.* 20(11): 1140-1143.